Catalysis Letters Vol. 102, Nos. 3–4, August 2005 (© 2005)
DOI: 10.1007/s10562-005-5852-8

Effect of steam and carbon dioxide pretreatments on methane decomposition and carbon gasification over doped-ceria supported nickel catalyst

Ta-Jen Huang* and Tien-Chun Yu

Department of Chemical Engineering, National Tsing Hua University, Hsinchu, Taiwan, 300 ROC

Received 4 February 2005; accepted 18 March 2005

Effects of steam (H_2O) and carbon dioxide (CO_2) pretreatments on methane (CH_4) decomposition and carbon gasification over doped-ceria supported nickel catalysts have been studied from 400 to 500 °C. The doped ceria employed were gadolinia-doped ceria and samaria-doped ceria. Results indicate that a drastic increase of both H_2O and CO_2 dissociation activities occurs as the temperature increases from 450 to 500 °C. The formation of the surface hydroxyl species during H_2O treatment inhibits the followed CH_4 decomposition. CO but no CO_2 was formed during CH_4 reaction after H_2O treatment. Carbon deposition during CH_4 decomposition is quite large but can be removed *via* gasification with afterward CO_2 treatment. However, some of the deposited carbon species is in a form which can not be removed with CO_2 treatment but can be removed with O_2 treatment. And, higher values of the oxygen-ion conductivity and the density of the surface oxygen vacancies lead to higher activities for all dissociation and decomposition reactions.

KEY WORDS: steam; carbon dioxide; pretreatment; methane decomposition; carbon gasification; doped ceria; nickel catalyst.

1. Introduction

Methane decomposition over the nickel catalyst is well known for the associated phenomenon of carbon deposition (coking) [1], which may lead to serious deactivation of the catalyst. However, it is also known that the deposited carbon can be removed *via* gasification by steam [2] or carbon dioxide [3]. For methane reactions, the nickel catalyst has been found to exhibit promising catalytic performance for steam reforming of methane [4,5] or carbon dioxide reforming of methane [6–8].

Oh et al. [9] reported that the steam reforming of methane over the alumina supported nickel catalyst was remarkably deactivated by steam treatment, which was attributed to the formation of $NiAl_2O_4$. In addition, Matsumura and Nakamori [5] reported that the activity of steam reforming of methane over nickel supported on silica decreases with oxidation of nickel particles by steam. On the other hand, the doped-ceria supported nickel catalyst exhibits much higher activity for steam reforming of methane than that of the alumina supported one [10]. For carbon dioxide reforming of methane, the doped-ceria supported nickel catalysts have also been observed to show high activities [3,11,12]. Thus, it looks interesting to investigate the effects of steam as well as carbon dioxide treatments on the methane reaction over doped-ceria supported nickel catalysts.

* To whom correspondence should be addressed.
E-mail: tjhuang@che.nthu.edu.tw

In addition, Matsumura and Nakamori [5] also reported that, during methane reaction after steam treatment, appreciable amount of carbon dioxide was formed over Ni/ZrO_2 catalyst at 500 °C. They proposed that the formation of carbon dioxide was due to the methane reaction with the hydroxyl group formed during steam treatment; reaction mechanism with separate feed of methane and steam was thus proposed. In this work, preliminary results indicate that, at 400–500 °C, CO but no CO_2 was formed during methane reaction after steam treatment, indicating different reaction mechanism from the above one. Therefore, it is also interesting to investigate the reaction mechanisms with separate feed of steam, carbon dioxide, and methane over the doped-ceria supported nickel catalysts.

In this work, steam and carbon dioxide pretreatments over doped-ceria supported nickel catalysts were carried out separately and its effects on methane decomposition as well as the gasification of the formed carbon species were investigated and compared at temperatures of 400–500 °C. The reaction mechanisms for all dissociation and decomposition reactions were also clarified and applied to explain the observed phenomena.

2. Experimental

2.1. Preparation of doped ceria

Gadolinia-doped ceria (GDC) was prepared by a co-precipitation method from reagent-grade (99.999% purity, Strem Chemical) metal nitrates $Gd(NO_3)_3{\cdot}6H_2O$

and $Ce(NO_3)_3{\cdot}6H_2O$. Appropriate amounts of gadolinium nitrate and cerium nitrate, corresponding to an atomic molar ratio of Gd:Ce = 1:9, were dissolved in de-ionized water to make 0.08 M solutions. Hydrolysis of the metal salts to hydroxides was obtained by slowly dropping each such solution into NH_4OH solution and in the meantime stirring to keep the pH of the solution >9. A distinct deep purple color of precipitate/gel was formed when the nitrate solution was dropped into NH_4OH. Vacuum filtration was employed to isolate the gel, which was then washed twice by water and ethanol. After washing, the gel was dried under vacuum at 110 °C for 4 h, calcined in air at 300 °C for 2 h and then at 600 °C for 4 h, and then slowly cooled down to room temperature.

Samaria-doped ceria (SDC) was prepared with the same method. The atomic molar ratio of Sm:Ce for SDC was also 1:9.

2.2. Preparation of doped-ceria supported nickel catalyst

The doped-ceria supported nickel catalyst was prepared by impregnating the above-prepared doped ceria with an appropriate amount of aqueous solution of nickel nitrate trihydrate, $Ni(NO_3)_2{\cdot}3H_2O$ (99.999% purity, SHOWA, Japan) for 7 h. After evaporating excess water at 80 °C (this is equivalent to impregnation to incipient wetness), the catalysts were dried under vacuum at 80 °C for 12 h, and then calcined in air at 260 °C for 1.5 h and then at 500 °C for 3.5 h. The calcination of the supported nickel catalyst was conducted by passing air at a rate of 1 L/min, and by ramping the temperature at a rate of 10 °C/min.

In this work, the nickel catalyst is always supported and with a loading of 2 wt% with respect to the weight of the support.

2.3. Activity test

The activity tests were conducted at 400∼500 °C under atmospheric pressure in a continuous flow reactor charged with 30 mg of sample, which was fixed by quartz wool and quartz sand downstream of the bed. The reactor was made of an 8-mm-ID quartz U-tube imbedded in an insulated electric furnace, equipped with a temperature programmable controller. A K-type thermocouple was inserted into the catalyst bed to measure and control bed temperature. All catalysts were pre-reduced at 500 °C in 25 mL/min of hydrogen for 30 min and then the reactor was purged with 75 mL/min of argon, also at 500 °C, for 30 min before the test.

After a specific temperature of the reactor is reached and stabilized in flowing argon, the test started with 30 min of steam or carbon dioxide feed, at 100 mL/min total with 25 mL/min of steam or carbon dioxide and balance argon, followed by 30 min of 75 mL/min argon flow for purging. Then, methane flowed for 30 min, at 100 mL/min of CH_4: Ar = 25:75, followed by 30 min of argon flow for purging. Then, carbon dioxide flowed for 120 min, at 100 mL/min of CO_2 : Ar = 25 : 75, followed by 30 min of argon flow for purging while the temperature was increased to 500 °C. Then, oxygen flowed for 30 min, at 100 mL/min of O_2 : Ar = 25 : 75. The product gases were measured on-line with a CO-NDIR (Beckman 880) and two gas chromatographs (China Chromatograph 8900, Taiwan).

3. Results and discussion

3.1. Characterization of support and catalyst

The surface areas of the supports are presented in table 1. It is seen that the surface areas of GDC and SDC are roughly the same, especially if considering only the external surface area which is obtained by deducting the micro-pore area from the total surface area as shown in table 1. Note that the micro-pore area has lower effectiveness for the catalytic reaction than the external surface area due to its pore size being in the nm range as shown in table 1. Also note that there is no macro-pore area for the supports of CeO_2, GDC, and SDC as shown in table 1 since the as-prepared fine powders with zparticle diameter <10 μm were used.

Huang and Kung [13] has reported that, in their temperature-programmed reduction (TPR) profiles, there is a peak at around 530 °C for yttria-doped ceria (YDC) when there is no metal loading; however, with 1 wt% copper loaded, the 530 °C peak disappears. They attributed the existence of this phenomenon to be due to the surface capping oxygen becoming a shared oxygen on CuO/YDC. They also note that the occurrence of the 530 °C peak is due to the surface capping oxygen of YDC. In our laboratory, we performed TPR tests over SDC, the SDC-supported 1 wt% Cu catalyst, and the SDC-supported 1 wt% and 2 wt% Ni catalysts; results showed the same phenomenon as that of Huang and Kung [13], i.e. a large peak at 550 °C for the surface capping oxygen of SDC disappears and these oxygen species contribute to the metal oxide (CuO or NiO) peak at 250–400 °C. As a consequence, the metal oxide peak becomes much larger than it should be if without the contribution of the surface capping oxygen. Thus, the specific surface area of the doped-ceria supported nickel may not be measured in accuracy by the traditional

Table 1
Surface areas of the supports[a]

Support	Total surface area (m^2/g)	Micro-pore area (m^2/g)	Average pore size (nm)
CeO_2	47	7	4.6
GDC	42	5	4.6
SDC	38	2	7.2
$\alpha-Al_2O_3$	6.3	–	–

[a]All these supports were calcined at 600 °C.

method of applying hydrogen. Note that the surface capping oxygen comes with the surface oxygen vacancies of ceria and the doped ceria; since the traditional support of alumina generally does not have the surface oxygen vacancies, the specific surface area of the alumina supported Ni catalyst should be able to be measured in better accuracy by the traditional method of applying hydrogen.

For comparison purpose, whether there is a difference in the specific surface areas may be tested with a model reaction since the specific surface area is directly related to the catalytic activity. In this work, we carried out the carbon dioxide reforming of methane, which consists of two main reactions in this work, i.e. methane and CO_2 reactions, to compare the activities of various supported Ni catalysts and the results are shown in figure 1. It is seen that, at temperatures below 400 °C, the activities of CeO_2, SDC, and GDC are almost the same. This may indicate that their specific surface areas are about the same.

It is also seen in figure 1 that, for temperatures from 400 to 450 °C, the activities of the α-Al_2O_3 supported Ni catalyst are lower than those of ceria supported Ni catalysts; nevertheless, the difference between the activities of CeO_2 and α-Al_2O_3 supported Ni catalysts at 400 °C is about the same as that at 450 °C. This difference is considered to be due to the difference in the surface area as shown in table 1. On the other hand, at temperatures higher than 450 °C, this difference becomes larger as the temperature increases. This phenomenon is considered to be due to the oxygen-ion conductivity of ceria and doped ceria [10] since alumina generally does not have oxygen-ion conductivity; in addition, the oxygen-ion conductivity increases as the temperature increases and this seems to be the major difference of ceria and doped ceria with alumina.

3.2. *Effect of steam pretreatment*

Figure 2 shows the results of steam (H_2O) pretreatment over Ni/GDC. It is seen that, during methane (CH_4) feeding, the amount of carbon monoxide (CO) formed at 450 °C is about the same as that at 400 °C but a drastic increase occurs as the temperature increases from 450 to 500 °C. This is the same behavior as those of the H_2O and carbon dioxide (CO_2) dissociation rates as presented in table 2. The drastic increase of the H_2O or CO_2 dissociation rate is considered to be due to the increase of the oxygen-ion conductivity with temperature. As the reaction temperature increases from 450 to 500 °C, the oxygen-ion conductivity becomes high enough so as to make the lattice oxygen mobile; thus, the lattice oxygen can be transported onto the surface or vice versa to affect the reaction kinetics. As the surface oxygen species is transported into the lattice, the H_2O or CO_2 dissociation rate is enhanced; and as the lattice oxygen is transported onto the surface, the CH_4 reaction rate is enhanced. These enhancement effects will be clarified with the following analyses of the mechanisms of the H_2O, CH_4, and CO_2 reactions.

For the reaction of H_2O dissociation, since the doped-ceria supported nickel catalyst has been reduced before the activity test in this work, the reaction may be considered to be the same as that over the reduced ceria [14] or Ni [15], both being the same, i.e.

$$H_2O + {}^* \rightarrow H_2 + O^* \qquad (1)$$

where * denotes an active site over nickel or a surface oxygen vacancy over ceria or is considered as an active site over the reduced ceria, and O* denotes an adsorbed oxygen species over nickel or an occupied oxygen vacancy or is considered as an oxidized ceria species [16]. According to reaction (1), as the surface oxygen species is transported into the lattice, the H_2O dissociation activity is enhanced. Thus, when the reaction temperature increases from 450 to 500 °C, the drastic increase of the H_2O dissociation rate as shown in table 2 is an indication that the lattice oxygen becomes mobile and so a large amount of the surface oxygen species can be transported into the lattice to increase the activity of reaction (1) drastically.

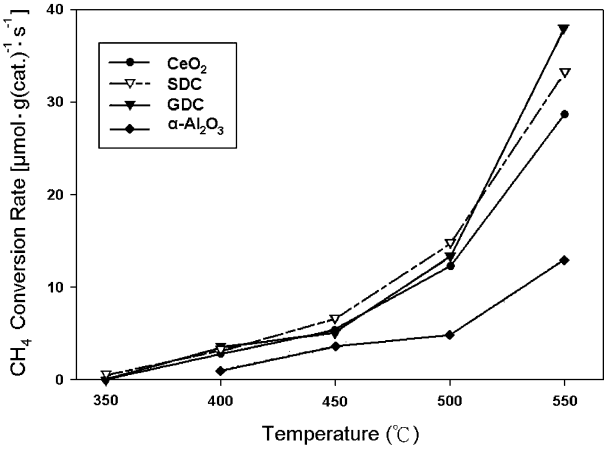

Figure 1. Methane conversion rate for CO_2 Reforming of methane. Feed: 100 mL/min of CH_4:CO_2:Ar = 25:25:50.

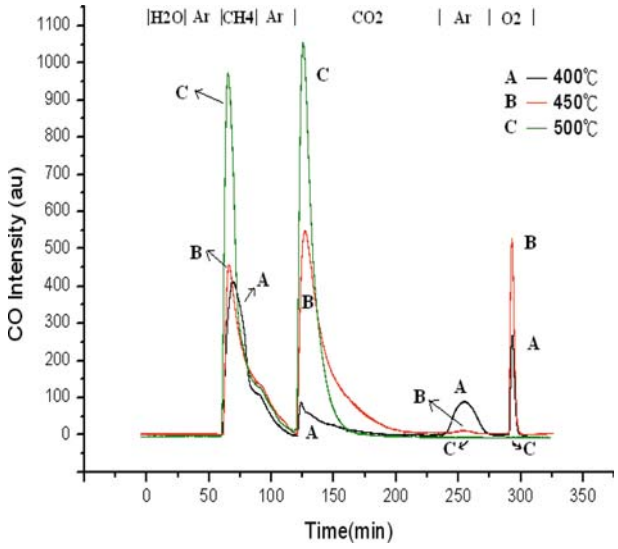

Figure 2. CO production profile for steam pretreatment over Ni/GDC.

Table 2
Average rate [a] (μmol/min) during 30 min of feeding. Pretreatment and methane decomposition at the specific temperature [b]

Pretreatment	Steam		Carbon dioxide	
Catalyst	Ni/GDC	Ni/SDC	Ni/GDC	Ni/SDC
400 °C				
H_2O dissociation[c]	0.60	0.53		
H_2 production from H_2O	0.51	0.48		
CO_2 dissociation[d]			0.68	0.62
CH_4 decomposition[e]	2.12	2.08	2.49	2.47
H_2 production from CH_4	4.12	4.02	4.97	4.88
450 °C				
H_2O dissociation	0.60	0.60		
H_2 production from H_2O	0.53	0.53		
CO_2 dissociation			0.68	0.65
CH_4 decomposition	2.22	2.15	3.82	2.98
H_2 production from CH_4	4.30	4.08	7.52	5.84
500 °C				
H_2O dissociation	1.07	1.03		
H_2 production from H_2O	0.99	0.96		
CO_2 dissociation			1.13	0.93
CH_4 decomposition	3.73	3.70	4.55	4.33
H_2 production from CH_4	7.27	7.19	8.99	8.44

[a]Average rate is obtained by first calculating the sum (in μmol) of conversion with the numerical trapezoidal method and then dividing the sum with the total time (in minutes) of conversion. The gas chromatographic measurement is done every 10 min.
[b]Feed concentrations of H_2O, CO_2, and CH_4 are the same at 10.23 μmole/mL.
[c]Average rate for H_2O dissociation is obtained during the initial 30 min (the H_2O feeding period) as shown in figures 2 and 3.
[d]Average rate for CO_2 dissociation is obtained during the initial 30 min (the CO_2 feeding period) as shown in figure 4.
[e]Average rate for CH_4 decomposition is obtained from 60 to 90 min (the CH_4 feeding period) as shown in figures 2–4.

As seen in table 2, during 30 min of steam pretreatment, the average rates of H_2O dissociation are all higher than those of hydrogen (H_2) production from H_2O dissociation. This is an indication that a reaction other than reaction (1) also occurs. During H_2O dissociation over the oxidized ceria, the hydroxyl species is formed according to the following reaction [17]:

$$H_2O + {}^* + O^* \rightarrow 2HO^* \quad (2)$$

The difference between H_2O dissociation rate and H_2 production rate may thus be an indication of the formation and the existence of the surface hydroxyl species which occupies the surface oxygen vacancy, at temperatures of 400–500 °C, i.e. the temperature range of this work. Note that the hydroxyl species may also be formed over Ni but decomposed at temperatures over 300 K [15].

As also seen in table 2, the average rates of H_2 production from CH_4 are all lower than trice those of the corresponding CH_4 decomposition. Since a complete decomposition of methane is $CH_4 = C + 2\ H_2$, this observation means that the following reaction occurs ($x \geq 0$) for methane decomposition:

$$CH_4 + {}^* \rightarrow CH_x^* + 1/2(4-x)H_2 \quad (3)$$

On the other hand, the formation of CO during CH_4 feeding is an indication of the oxidation of some carbon species, which is considered to be the CH_x ($x \geq 0$) species here. Thus, the CH_x species is simultaneously removed from the surface according to the following reaction ($x \geq 0$):

$$CH_x^* + O^* \rightarrow CO + x/2H_2 + 2^* \quad (4)$$

Note that, during CH_4 reaction over doped-ceria supported Ni catalyst, CO but no CO_2 was formed either without H_2O pretreatment [18] or with H_2O pretreatment as observed in this work at temperatures of 400–500 °C.

The O species needed in reaction (4) may be those produced from H_2O *via* reaction (1) during the previous period of H_2O feeding, or be supplemented from the lattice oxygen; the latter is correspondent to the above-described drastic activity increase. As the reaction temperature increases from 450 to 500 °C, a drastic increase of the O species may occur if the lattice oxygen becomes mobile and thus the O species may be supplemented from the lattice. As a consequence, the activity of reaction (4) and thus that of reaction (3) can increase drastically. This is in agreement with the observation of the drastic increase of the CH_4 decomposition rate as shown in table 2.

As seen in figure 2, during argon (Ar) purging after CH_4 feeding, CO is formed continuously for about 30 min. This is an indication of carbon deposition (coking), and also the oxidation of the deposited carbon species during this period of Ar purging. The oxygen species needed for this oxidation may also be those produced from H_2O *via* reaction (1) during the period of H_2O feeding, or be supplemented from the lattice oxygen as described above.

As also seen in figure 2, after CO_2 is introduced, a large peak of CO is formed. This indicates that the amount of the deposited carbon after CH_4 feeding is quite large, i.e. a serious coking problem, and the oxidation of the deposited carbon species during the following Ar purging period removes only a small portion of it. Since CO formation has decreased to nearly zero at the end of the Ar purging period, indicating that the available oxygen species has been almost completely consumed, the large amount of the O species needed here should have been supplied by CO_2 dissociation. To supply the O species needed for the oxidation of the deposited carbon species, CO_2 dissociation is considered to occur as the following:

$$CO_2 + {}^* \rightarrow CO + O^* \quad (5)$$

As the surface oxygen species is transported into the lattice, the activity of reaction (5) is enhanced. Thus, when the reaction temperature increases from 450 to 500 °C, the drastic increase of the CO_2 dissociation rate as shown in table 2 is an indication that the lattice oxygen becomes mobile and so a large amount of the surface oxygen species can be transported into the lattice to increase the activity of reaction (5) drastically.

As also seen in figure 2, during Ar purging after CO_2 treatment, CO evolves. Since CO has ceased to be formed at the end of the period of CO_2 after-treatment, the appearance of the CO peak during the followed period of Ar purging should be due to pre-adsorbed CO. This CO peak is larger at lower reaction temperature indicating that CO adsorption over the doped-ceria supported Ni catalyst is stronger at lower temperature.

Figure 3 shows the results of steam pretreatment over Ni/SDC. It is seen that the CO production profile over Ni/SDC is similar to that over Ni/GDC as shown in figure 2. Nevertheless, during CH_4 feeding, the amount of CO formed over Ni/SDC is lower than that over Ni/GDC. In addition, table 2 shows that the rate of CH_4 decomposition over Ni/SDC is lower than that over Ni/GDC. These observations indicate that the activity of Ni/SDC is lower than that of Ni/GDC. Since the density of the surface oxygen vacancies of SDC is lower than that of GDC [10], the amount of the interfacial active center of Ni–oxygen vacancy over Ni/SDC is lower than that over Ni/GDC. As a consequence, a lower activity of Ni/SDC than that of Ni/GDC is observed as indicated above. This is an indication that the interfacial active center of Ni–oxygen vacancy plays an important role in CH_4 decomposition.

The above-described result of CO_2 after-treatment is a demonstration of the carbon removal (de-coking) ability of CO_2. Nevertheless, as seen in figures 2–4, at the end of CO_2 treatment, CO formation has come to nearly zero indicating that the CO_2 de-coking reaction does not occur any more. On the other hand, with oxygen treatment at 500 °C, CO is still formed even after CO_2 treatment at 500 °C, indicating some residual carbon species after CO_2 treatment. Thus, some of the deposited carbon species should be in a form which can not be removed with CO_2 treatment but can be removed with O_2 treatment.

3.3. *A comparison of steam and carbon dioxide pretreatments*

Table 2 shows that the CH_4 decomposition rates after CO_2 pretreatment are all much higher than those after H_2O pretreatment. Since the catalyst and the reaction temperature are exactly the same, this large difference in the CH_4 decomposition rate should thus be due to some differences on the surface modification after CO_2

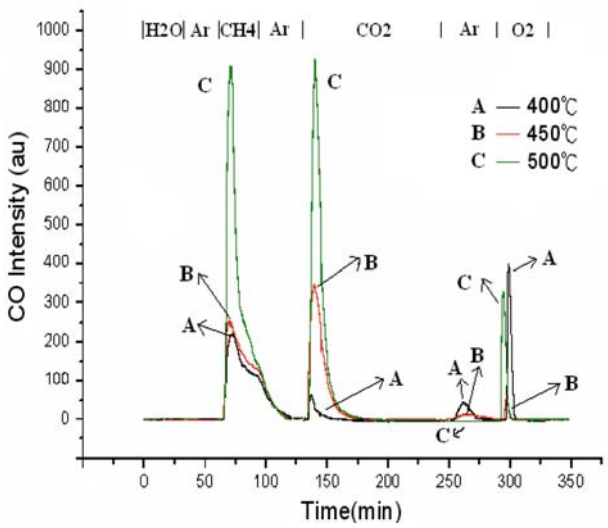

Figure 3. CO production profile for steam pretreatment over Ni/SDC.

pretreatment from that after H_2O pretreatment. From the above discussions, one difference is very possibly the existence of the surface hydroxyl species which occupies the surface oxygen vacancy after H_2O pretreatment. The formation of the surface hydroxyl species which occupies the surface oxygen vacancy will not only decrease the amount of the oxygen species formed but also decrease the availability of the surface oxygen vacancy for the formation of the interfacial active center of Ni–oxygen vacancy. Therefore, the existence of the surface hydroxyl species which occupies the surface oxygen vacancy decreases not only the rate of reaction (4) but also the rate of reaction (3). As a consequence, the CH_4 decomposition activity decreases. The lower CH_4 decomposition rates after H_2O pretreatment is thus an indication of the inhibition effect of the surface hydroxyl species.

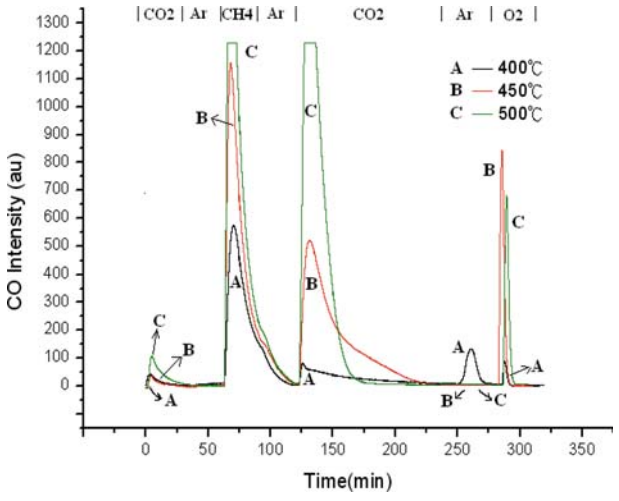

Figure 4. CO production profile for carbon dioxide pretreatment over Ni/GDC.

Another difference on the surface modification after CO_2 pretreatment from that after H_2O pretreatment may be the density of the surface oxygen species. This is demonstrated by that, at 400 and 450 °C, the CO_2 dissociation rates are higher than the H_2O dissociation rate and thus the densities of the surface oxygen species after CO_2 pretreatment are higher than those after H_2O pretreatment, according to reactions (1) and (5). According to reactions (3) and (4), a higher density of the surface oxygen species should lead to a higher CH_4 decomposition rate.

A comparison of figures 2 and 4 shows that, during CH_4 feeding and as the reaction temperature increases from 400 to 450 °C, the amount of CO formed is about the same after H_2O pretreatment but it has a large difference after CO_2 pretreatment, i.e. the amount of CO formed at 450 °C is much larger than that at 400 °C. Since CO is formed *via* the oxidation of the carbon species, which is produced by CH_4 decomposition, higher CH_4 decomposition rate produces higher concentration of the carbon species and thus larger amount of CO is formed. Thus, the much larger amount of CO corresponds to the much higher rate of CH_4 decomposition.

As also seen in table 2, at 400 and 450 °C over Ni/GDC, the H_2O dissociation rates are identical and the followed CH_4 decomposition rates are quite close; on the other hand, the CO_2 dissociation rates are also identical but the followed CH_4 decomposition rate at 450 °C is much higher than that at 400 °C. This difference can also be attributed to the inhibition effect of the surface hydroxyl species, which results in lower densities of both the surface oxygen species and the surface oxygen vacancies after H_2O pretreatment. Thus, the density of the interfacial active center of Ni–oxygen vacancy after CO_2 pretreatment is higher than that after H_2O pretreatment. Since methane is

adsorbed only onto Ni, the interfacial active center of Ni–oxygen vacancy should be important for the methane reaction to take advantage of the oxygen species produced over the doped ceria. Note that the oxygen species is considered to migrate *via* the oxygen vacancies over the doped ceria. Since the oxygen species may diffuse or migrate over all surfaces, the increase of the diffusivity of the oxygen species due to increasing temperature should increase the availability of the oxygen species at the interfacial active center and thus should increase the methane activity if the density of the interfacial active center is the same. As a consequence, higher density of the interfacial active center coupled with higher density of the surface oxygen species after CO_2 pretreatment than those after H_2O pretreatment lead to the above-described much higher CH_4 dissociation rate.

As also shown in table 2, at 450 °C, the CH_4 dissociation rate over Ni/SDC is slightly lower than that over Ni/GDC after H_2O pretreatment, but it is much lower after CO_2 pretreatment. This much lower CH_4 decomposition rate over Ni/SDC than that over Ni/GDC can also be attributed to the above-described lower density of the surface oxygen vacancies of SDC than that of GDC. According to the above discussions, the resulting lower density of the interfacial active center of Ni–oxygen vacancy over Ni/SDC can lead to the much lower CH_4 decomposition rate as observed. This indicates the importance of the density of the surface oxygen vacancies on the methane activity and thus the surface hydroxyl species which occupies the surface oxygen vacancy can inhibit the methane dissociation rate greatly.

Nevertheless, although the oxygen-ion conductivity may be too low to affect the activity at temperatures of 450 °C or lower [10], it will affect the activity when the temperature increases to 500 °C as described above. As a consequence, at 500 °C, the higher oxygen-ion conductivity of SDC than that of GDC [10] may compensate for the lower density of the surface oxygen vacancies of SDC and thus the activities of Ni/SDC and Ni/GDC become close to each other, as shown in table 2 for the CO_2-pretreatment case.

It is also seen in table 2 that, as the reaction temperature increases from 450–500 °C, the extent of the increase of the H_2O dissociation rate is larger than that of the CO_2 dissociation rate, especially over Ni/SDC which even results in a higher H_2O dissociation rate than the CO_2 dissociation rate. As a consequence, the extent of the increase of the CH_4 decomposition rate after H_2O pretreatment is larger than that after CO_2 pretreatment. This may be an indication that the higher oxygen-ion conductivity at 500 °C may decrease the inhibition effect of the surface hydroxyl species just as the above case of higher oxygen-ion conductivity of SDC may compensate for its lower density of the surface oxygen vacancies.

4. Conclusions

(1) A drastic increase of both H_2O and CO_2 dissociation activities occurs as the temperature increases from 450 to 500 °C.
(2) The formation of the surface hydroxyl species during H_2O dissociation inhibits the followed CH_4 decomposition.
(3) CO but no CO_2 was formed during CH_4 reaction after H_2O treatment.
(4) CO is adsorbed onto the doped-ceria supported Ni catalyst and its adsorption is stronger at lower temperature.
(5) Some of the deposited carbon species is in a form which can not be removed with CO_2 treatment but can be removed with O_2 treatment.
(6) Higher oxygen-ion conductivity of SDC than that of GDC may compensate for the lower density of the surface oxygen vacancies of SDC.

Acknowledgments

The assistance of Mr. Han-Chun Lin in the characterization of support and catalyst is acknowledged.

References

[1] M.A. Ermakova, D.Y. Ermakov, G.G. Kuvshinov and L.M. Plyasova, J. Catal. 187 (1999) 77.
[2] V.R. Choudhary, S. Banerjee and A.M. Rajput, Appl. Catal. A 234 (2002) 259.
[3] J.B. Wang, Y.S. Wu and T.J. Huang, Appl. Catal. A 272 (2004) 289.
[4] H.S. Roh, K.W. Jun, W.S. Dong, J.S. Chang, S.E. Park and Y.I. Joe, J. Mol. Catal. A 181 (2002) 137.
[5] Y. Matsumura and T. Nakamori, Appl. Catal. A 258 (2004) 107.
[6] M.J. Hei, H.B. Chen, J. Yi, Y.J. Lin, Y.Z. Lin, G. Wei and D.W. Liao, Surf. Sci. 417 (1998) 82.
[7] A.A. Lemonidou and I.A. Vasalos, Appl. Catal. A 228 (2002) 227.
[8] Z. Hao, H.Y. Zhu and G.Q. Lu, Appl. Catal. A 242 (2003) 275.
[9] Y.S. Oh, H.S. Roh, K.W. Jun and Y.S. Baek, Internat. J. Hydro. Energy 28 (2003) 1387.
[10] T.J. Huang, H.C. Lin and T.C. Yu, Appl. Catal. A, submitted (2004).
[11] J.B. Wang, Y.L. Tai, W.P. Dow and T.J. Huang, Appl. Catal. A 218 (2001) 69.
[12] J.B. Wang, S.Z. Hsiao and T.J. Huang, Appl. Catal. A 246 (2003) 197.
[13] T.J. Huang and Y.C. Kung, Catal. Lett. 85 (2003) 49.
[14] E. Ramirez-Cabrera, A. Atkinson and D. Chadwick, Appl. Catal. B 47 (2004) 127.
[15] R.V. Kasza, K. Griffiths, J.G. Shapter, P.R. Norton and D.A. Harrington, Surf. Sci. 356 (1996) 195.
[16] S. Sharma, S. Hilaire, J.M. Vohs, R.J. Gorte and H.W. Jen, J. Catal. 190 (2000) 199.
[17] G. Jacobs, E. Chenu, P.M. Patterson and L. Williams, Appl. Catal. A 258 (2004) 203.
[18] H.C. Lin, M.S. Thesis, National Tsing Hua University,Taiwan, ROC (2004) p. 38.